Operation of GaN Planar Nanodiodes as THz Detectors and Mixers

Ignacio Íñiguez-de-la-Torre, Carlos Daher, Jean-François Millithaler, Jérémi Torres, Philippe Nouvel, Luca Varani, Paul Sangaré, Guillaume Ducournau, Christophe Gaquière, Tomás González, *Senior Member, IEEE*, and Javier Mateos, *Member, IEEE*

***Abstract*—In this paper, we perform, by means of Monte Carlo simulations and experimental measurements, a geometry optimization of GaN-based nano-diodes for broadband Terahertz direct detection (in terms of responsivity) and mixing (in terms of output power). The capabilities of the so-called self-switching diode (SSD) are analyzed for different dimensions of the channel at room temperature. Signal detection up to the 690 GHz limit of the experimental set-up has been achieved at zero bias. The reduction of the channel width increases the detection responsivity, while the reduction in length reduces the responsivity but increases the cut-off frequency. In the case of heterodyne detection an intrinsic bandwidth of at least 100 GHz has been found. The intermediate frequency (IF) power increases for short SSDs, while the optimization in terms of the channel width is a trade-off between a higher non-linearity (obtained for narrow SSDs) and a large current level (obtained for wide SSDs). Moreover, the RF performance can be improved by biasing, with optimum performances reached, as expected, when the DC non-linearity is maximum.**

***Index Terms*—Mixing, Monte Carlo simulations, nanoelectronics, rectification, terahertz science.**

I. Introduction

THE range of the electromagnetic spectrum commonly referred to as "Terahertz gap" is still missing devices able to boost the availability of applications that the market requires nowadays. Among the candidates, like Schottky diode-based detectors [1] or THz transistors [2], we report on a unipolar device, known as self-switching diode (SSD). Originally proposed by A. M. Song [3], GaAs-based SSDs have already shown experimentally a good responsivity of 300 V/W at 1.5 THz at room temperature [4]; and noise equivalent power of 65 pW/$\sqrt{\text{Hz}}$ at 110 GHz [5] in the case of InGaAs-based SSDs. This paper is a follow up of two prior works where the capabilities of SSDs based on an AlGaN/GaN heterostructure operating as detectors [6] and mixers [7] have been experimentally demonstrated. Even if III-V narrow band-gap materials like InAs [8] or InSb [9] are more suitable for THz applications, in this work the choice of GaN has been made because SSDs based on this semiconductor are theoretically expected to be able to generate sub-millimeter wave oscillations based on Gunn effect [10]. In this context, our final target is to design a simple, compact, room temperature, continuous wave, tunable and powerful integrated sub-THz emitter/detector system within the same material.

The use of GaN nanodiodes as sub-THz detectors is fairly new but with a lot of room for improvement to make SSDs competitive as compared to the mainstream technologies (Schottky barrier diodes [11], [12] and bolometers [13]) and promising recent developments (plasma detection with Si MOSFETs [14] and Sb-based backward diodes [15]). Indeed, up to now our highly resistive devices have not been designed to achieve an optimum power matching. On the other hand, the capability of GaN-based devices for high power handling is unparalleled by any other technology. We expect the widebandgap of this material to allow GaN SSDs being used as ultra-high power RF detectors. Moreover, the planar geometry and the ease of fabrication make SSDs highly competitive in the prospect of a new generation of room temperature sub-THz detectors. Finally, to overcome the high impedance of the SSDs many of them in parallel are typically employed to minimize the mismatch loss.

The aim of this paper is to present a systematic numerical study, based on an in-house Monte Carlo (MC) simulator, of the performance of such GaN nanodiodes as direct and heterodyne detectors as a function of their geometry and bias conditions supported and validated with experimental measurements. The paper is organized as follows. Section II introduces the geometries of the different SSDs, the experimental set-ups and the results of the DC simulations along with the measurements for calibration of the MC model. The dynamic performance at high frequency is reported, first, in Section III for the direct detection scheme and, later, in Section IV for the heterodyne one. Some conclusions are finally given in Section V.

Manuscript received June 06, 2014; revised July 21, 2014; accepted August 25, 2014. Date of publication September 16, 2014; date of current version October 30, 2014. This work was supported in part by the European Commission through the ROOTHz under Project ICT-2009-243845, by the Direccion General de Investigación (MICINN) and the Consejería de Educación de la Junta de Castilla y Leon under Projects TEC 2010-15413 and SA052U13, respectively, and by TERALAB Montpellier project, which received funding from the French Government and the Regional Council and has benefited of the facilities of Ex-CELSiOR-Nanoscience Characterization Center.

I. Íñiguez-de-la-Torre, J.-F. Millithaler, T. González, and J. Mateos are with the Department of Applied Physics, University of Salamanca, 37008 Salamanca, Spain (e-mail: indy@usal.es; jeff.millithaler@gmail.com; tomasg@usal.es; javierm@usal.es).

C. Daher, J. Torres, P. Nouvel, and L. Varani are with the Institut d'Electronique du Sud, UMR CNRS 5214, TeraLab, Université Montpellier 2, Montpellier, 34095, France (e-mail: daher@ies.univ-montp2.fr; jeremi.torres@ies.univ-montp2.fr; nouvel@ies.univ-montp2.fr; luca.varani@univ-montp2.fr).

P. Sangaré, G. Ducournau, and C. Gaquière are with the Institut d'Electronique de Microélectronique et de Nanotechnologie (IEMN), UMR CNRS 8520, Université de Lille 1, 59652, Villeneuve d'Ascq CEDEX, France (e-mail: pa.sangare@ed.univ-lille1.fr; guillaume.ducournau@iemn.univ-lille1.fr; christophe.gaquiere@iemn.univ-lille1.fr).

Color versions of one or more of the figures in this paper are available online at http://ieeexplore.ieee.org.

Digital Object Identifier 10.1109/TTHZ.2014.2356296

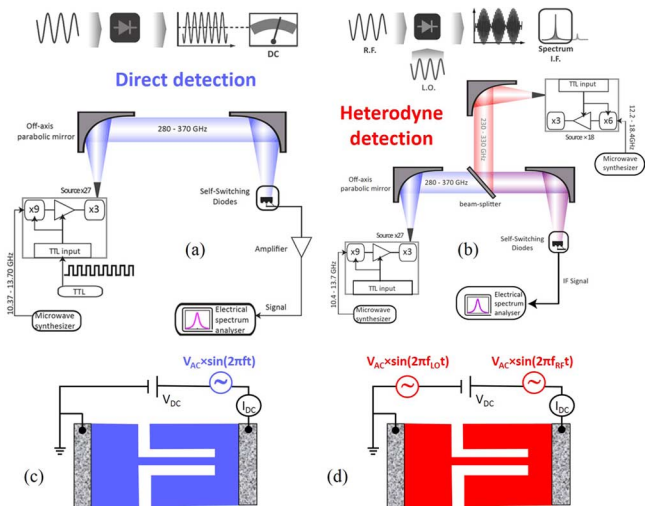

Fig. 1. Schematic diagrams for and experimental setup configuration for: (a) direct detection and (b) mixing or heterodyne detection (see [7]). The corresponding numerical framework are sketched in (c) and (d), respectively.

II. Device Under Test, Monte Carlo Simulations and Experimental Setup

The device under test consists of a narrow semiconductor channel with broken symmetry defined by L-shaped insulating trenches etched on a GaN heterostructure. The working operation of SSDs is based on the geometrical asymmetry and the presence of surface states at the sidewalls of the channel [16]. The two main design parameters are the length and the width of the channel, denoted as L and W. The width of the trenches and its filling material could also be considered for further optimization. Two different applications of the SSDs will be studied: 1) direct detection [Fig. 1(a)] and 2) heterodyne detection or mixing [Fig. 1(b)]. Figs. 1(c) and 1(d) shows the corresponding MC representation. In the first case, as a consequence of its non-linear response, when a device is irradiated with a RF wave, the voltage between the terminals of the SSDs has a DC component which is proportional to the power of the input signal, so that it can be used to perform direct detection. In the case of heterodyne detection, the signal carrying information (with a RF or THz carrier) is combined with the output of a local oscillator (LO, operating at a frequency near that of the carrier) using the device as a mixer. As a result, the output from the mixer has a component or contribution around an intermediate frequency (IF, equal to the difference between the LO and the original carrier) which is easier to amplify and work with than the original signal (it has much lower frequencies but contains all the information).

To include the THz radiation in the MC tool we just apply an oscillatory voltage to the contact, which represents the signal that is coupled through the integrated bow-tie antennas in the measurements performed in free space. To simulate the behavior of electrons in the device we make use of a semi-classical ensemble MC simulator self-consistently coupled with a 2D Poisson solver. Previous works demonstrate the validity of our model to explain not only the static but also the noise and dynamic properties of the SSD device [17]–[19].

Two sets of devices have been simulated, the first dedicated to the study of direct detection and the second to mixing properties. In order to perform the study of the dependence on L and W, of both direct and heterodyne detection, devices with: 1) constant L and different W and 2) constant W and different L have been simulated. The DC response of all of them is plotted in Fig. 2, showing the expected dependences with W and L and exhibiting good agreement with the available measurements of two devices, both with $L = 1$ μm, one with $W = 90$ nm (used for the demonstration of direct detection in [6]) and the other with $W = 150$ nm (used for heterodyne detection in [7]). It is to be noted that to obtain correct results we have employed a self-consistent model for the surface charge effects, recently implemented for GaN SSDs [10]. For the dimensions considered here, the static response, current level and impedance depend more significantly on the channel width than on the channel length. Note that the typical impedance is in the order of kΩ.

Once the DC response has been simulated and compared with values measured experimentally, in the next sections we provide design rules to optimize the performance of the GaN SSDs.

III. Direct Detection

The MC modelling of the direct detection is performed as follows. A sinusoidal signal of varying frequency is superimposed to the $V_{\rm DC}$ bias: $V(t) = V_{\rm DC} + V_{\rm AC}\cos(2\pi ft)$. The rectified current, $I_{\rm rect}(f)$, is obtained as the time-average value, $\overline{I(f)}$, of the instantaneous values of the current response $I(t)$ minus the DC current corresponding to the DC bias point $I_{\rm DC}$; $I_{\rm rect}(f) = \overline{I(f)} - I_{\rm DC}$. The matched or maximum, with an optimum lossless match, voltage responsivity, $R_m(f)$, is then determined by converting $I_{\rm rect}(f)$ into voltage, $V_{\rm rect}(f)$, by means of the resistance of the diode R_0 as $V_{\rm rect}(f) = R_0 \times I_{\rm rect}(f)$. Evaluating the active power dissipated at the matched SSD as $P_m(f) = {\rm Re}[(V_{\rm AC}^2)/(2Z(f))]$, one can obtain the frequency dependent impedance-matched responsivity as $R_m(f) = V_{\rm rect}(f)/P_m(f)$. $Z(f)$, see the inset of Fig. 3, is the frequency dependent complex impedance of the SSD, which has also been extracted from the MC simulation taking as a base the values of $I(t)$ (following [20]). The unmatched responsivity (when the device is connected to a line with characteristic impedance Z_0), $R_{\rm um}(f)$, is simply determined by exchanging $P_m(f)$ in the denominator by the delivered power $P_{\rm um}(f)$. Thus $R_{\rm um}(f) = V_{\rm rect}(f)/P_{\rm um}(f)$ with $P_{\rm um}(f) = P_m(f)/[1 - |\Gamma(f)|^2]$, obtained by using the reflection coefficient of the device, Γ, when inserted into the coplanar access line with characteristic impedance Z_0, $\Gamma(f) = [Z(f) - Z_0]/[Z(f) + Z_0]$. Note that the number of parallel SSDs has been taken into account for the calculation of the value of $\Gamma(f)$. Here we use the typical $Z_0 = 50$ Ω.

The unmatched MC results of direct detection at room temperature and equilibrium ($V_{\rm DC} = 0$ V) are presented in Fig. 3, where the good agreement with the on-wafer electrical experimental results of Ref. 6 for a single SSD with $L = 1.0$ μm and $W = 90$ nm can be observed. Reducing the width from 110 nm down to 50 nm significantly enhances the responsivity up to almost 300 V/W [Fig. 3(a)] at low frequency, as a result of more prominent surface effects that increase the non-linearity

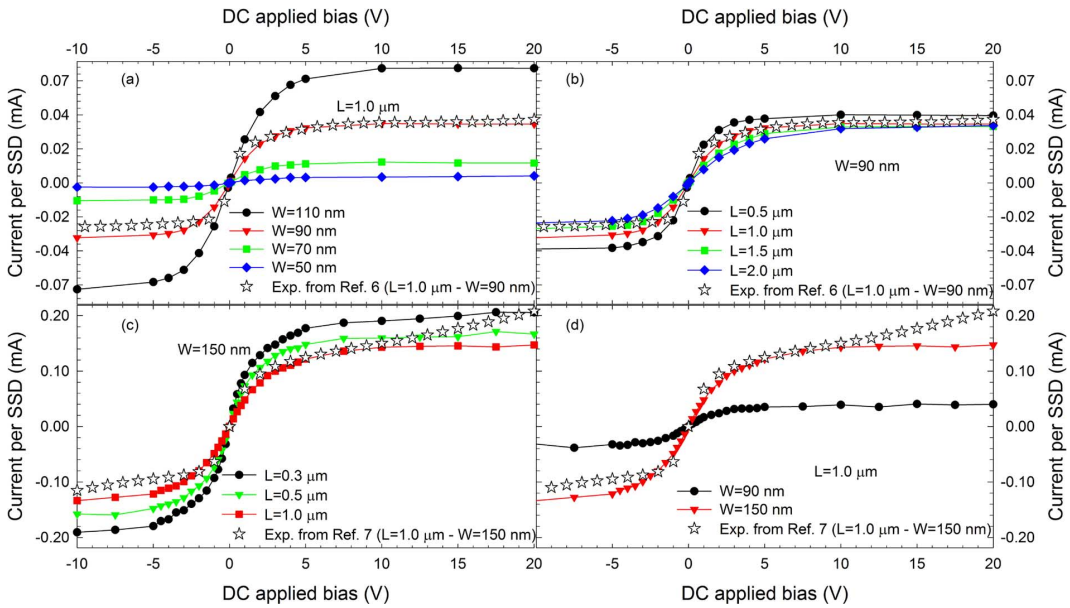

Fig. 2. Monte Carlo *I-V* curves of the SSDs used for the two types of experiments: direct detection (a) $L = 1.0\ \mu$m and $W = 110, 90, 70$ and 50 nm, and (b) $W = 90$ nm and $L = 0.5,\ 1.0,\ 1.5$ and $2.0\ \mu$m; and for mixing (c) $W = 150$ nm and $L = 0.3, 0.5$ and $1.0\ \mu$m and (d) $L = 1.0\ \mu$m, and $W = 90$ and 150 nm. The experimental results used to calibrate the simulations are taken form [6] and [7].

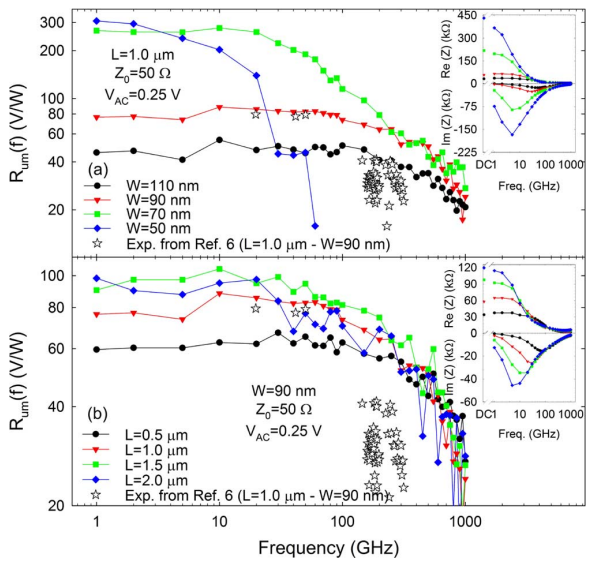

Fig. 3. Monte Carlo unmatched responsivity in V/W calculated for the devices of Fig. 2(a) and 2(b). In particular: (a) $L = 1.0\ \mu$m and $W = 110, 90, 70$ and 50 nm and (b) $W = 90$ nm and $L = 0.5,\ 1.0,\ 1.5$ and $2.0\ \mu$m. Insets show the frequency dependence of $Z(f)$ of each device. In all cases the simulations are performed for a single SSD at room temperature, with an excitation of $V_{\rm AC} = 0.25$ V, $V_{\rm DC} = 0$ V and considering a 50 Ω coplanar waveguide. The experimental values for $L = 1.0\ \mu$m and $W = 90$ nm are from [6].

of the *I-V* curve. On the other hand, the narrower the channel the higher frequency roll-off. A good compromise is found for $W = 70$ nm, providing a responsivity above 200 V/W up to almost 50 GHz. Moreover the noise behavior of the SSD with $W = 50$ nm is also significantly degraded by the sharp increase of the zero bias DC resistance R_0. Finally, acceptable values of tens of V/W are still expected beyond 0.5 THz. Fig. 3(b) shows how the responsivity slightly increases with L, while its frequency roll-off is stronger. In addition to the frequency dependence of the intrinsic response, the intrinsic impedance $Z(f)$ of the different SSDs (shown in the insets of Fig. 3) is responsible, in part, of the frequency behavior of the experimental responsivity and $R_{\rm um}(f)$ through the value of $\Gamma(f)$. Moreover, the parasitics (mainly the crosstalk capacitance) have also a significant influence on the high frequency behaviour of the responsivity, and we believe that it is at the origin of the disagreement between the experiments and MC results of Fig. 3.

In order to corroborate the predictions of MC simulations new free space detection measurements have been done using three tunable electronic sources from Virginia Diodes, Inc. based on a frequency-synthesizer whose input signal was multiplied by factors of 18, 27, and 49. The accessible frequencies ranges are 220–320 GHz, 280–380 GHz, and 640–690 GHz. The beam was chopped at 1 kHz using a TTL input. The beam is collimated using an off-axis parabolic mirror, and then it is focalized by means of a second parabolic mirror on our sample. The signal is amplified using a 40 dB amplifier, and measured by an electrical spectrum analyzer. A schematic of the setup is shown in Fig. 1(a). The SSDs are mounted on a FR7-holder where DC-lines are printed. In order to improve the noise equivalent power of the detectors [19], we designed each device as an array of 16 or 32 SSDs integrated within a single bow-tie antenna. The use of arrays not only reduces the voltage noise (as a consequence of a lower resistance) but also benefits the impedance matching due to the highly resistive character of the SSDs. The connection between the devices and the holder are ensured by gold-bonding, whereas connections with RF coaxial cables are made through SMA (SubMiniature version A) connectors.

Fig. 4(a) shows the results at zero bias ($V_{\rm DC} = 0$ V) for $L = 1.0$ and $0.5\ \mu$m and $W = 500$ and 700 nm in an arrangement of 32 SSDs in parallel. The responsivities are very small due to the large width of the SSDs but, interestingly, a tiny responsivity of about 0.1 mV/W has been recorded for frequencies

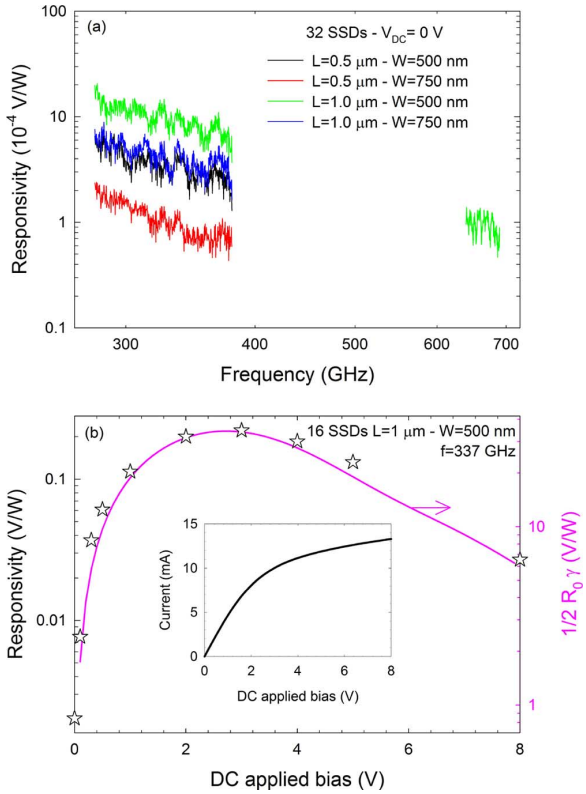

Fig. 4. (a) Experimental responsivity in V/W at equilibrium, measured to study the influence of the channel width and channel length is 32 SSDs with: $L = 1.0\ \mu\text{m} - W = 500$ nm, $L = 1.0\ \mu\text{m} - W = 750$ nm, $L = 0.5\ \mu\text{m} - W = 500$ nm and $L = 0.5\ \mu\text{m} - W = 750$ nm. (b) Bias dependence of the responsivity at 337 GHz for 16 SSDs with $L = 1.0\ \mu$m and $W = 500$ nm and curvature coefficient (right axis) corresponding to the $I(V)$ curve of the inset. In all cases, the measurements are in free space at room temperature and with 1 mW power of the source.

up to 690 GHz, which demonstrates the intrinsic capability of these devices to operate at such high frequencies. The plotted responsivity is directly calculated as the ratio between the induced voltage and the absolute power of the THz source. Since no normalization related to the areas of the radiation beam spot and the devices (which is very difficult to estimate and originates a lot of uncertainty) has been performed, the effective responsivities can be higher than those plotted in Fig. 4(a). In any case, we must remark that the efficiency of the power coupling between the free space radiation and the device antennas is quite low. Comparing these results with those obtained in guided measurements (with RF probes and coplanar waveguide accesses) in the same devices, we have estimated the efficiency loss of free space measurements to be roughly about -10 dB. This makes impossible the quantitative comparison with the MC results. However, the qualitative trend observed in the simulations (higher response for longer and narrower SSDs) is again confirmed by the free space experiments.

Finally, we have measured in free space, at a fixed frequency of 337 GHz, the responsivity as a function of the DC bias for 16 parallel SSDs with $L = 1.0\ \mu$m and $W = 500$ nm. The results of Fig. 4(b) show a strong enhancement of the responsivity when biasing the SSD, almost 2 orders of magnitude, with a maximum in the range 2–4 V, just in the knee of the *I-V* curve of the SSD [see inset of Fig. 4(b)], as expected from the well-known link

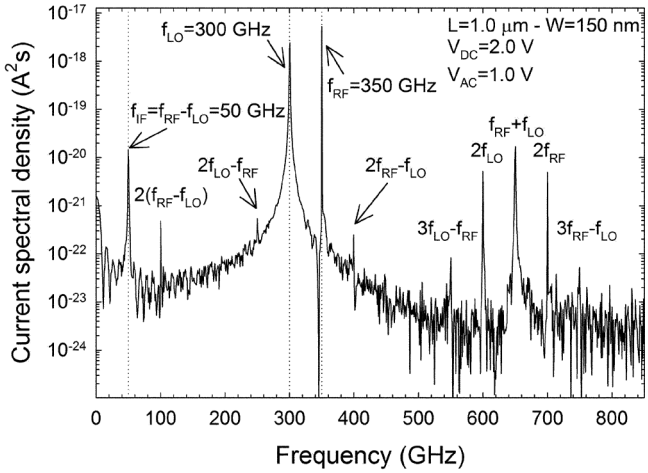

Fig. 5. Monte Carlo spectral density of the simulated current history in a SSD with $L = 1.0\ \mu$m and $W = 150$ nm. The frequency of the LO and RF signals are $f_{\rm LO} = 300$ GHz and $f_{\rm RF} = 350$ GHz, respectively, and the bias conditions are $V_{\rm DC} = 2.0$ and $V_{\rm AC} = 1.0$ V.

between the RF detection and the nonlinearity of the *I-V* curve. In fact, the measured values perfectly agree with the dependence of the theoretical matched responsivity [21], which is equal to $1/2R_0\gamma$, being R_0 the zero-bias resistance and γ the curvature of the *I-V* curve, defined as $\gamma = (d^2I/dV^2)/(dI/dV)$ [right axis of Fig. 4(b)].

IV. Heterodyne Detection

For the second set of simulations to analyze the mixing capabilities of the GaN-SSDs we use two sinusoidal signals with different frequencies, denoted $f_{\rm RF}$ and $f_{\rm LO}$, with the same amplitude on top of a DC bias. In the MC simulation we have access to the instantaneous values of the current between the two terminals, $I(t)$. By means of a fast Fourier transform (FFT) we can easily obtain its spectral density to determine the IF amplitude in devices with different geometries under diverse bias conditions. The frequency resolution, Δf, is given by the inverse of $Ni \times dt$, being Ni the number of MC iterations and dt the time step. Typically $dt = 1\ fs$ and $Ni = 10^6$, so that $\Delta f = 1$ GHz. Fig. 5 shows the current spectral density, $S_I(f)$, obtained with $f_{\rm LO} = 300$ GHz and $f_{\rm RF} = 350$ GHz, so that the IF is at 50 GHz $= f_{\rm RF} - f_{\rm LO}$. Other harmonics are also visible at frequencies $2(f_{\rm RF} - f_{\rm LO}) = 100$ GHz, $2f_{\rm LO} - f_{\rm RF} = 250$ GHz, $2f_{\rm RF} - f_{\rm LO} = 400$ GHz, $3f_{\rm LO} - f_{\rm RF} = 550$ GHz, $2f_{\rm LO} = 600$ GHz, $f_{\rm RF} + f_{\rm LO} = 650$ GHz, $2f_{\rm RF} = 700$ GHz and $3f_{\rm RF} - f_{\rm LO} = 750$ GHz. The dimensions of the SSD are $L = 1000$ nm and $W = 150$ nm, and the bias conditions are $V_{\rm AC} = 1.0\ V$ and $V_{\rm DC} = 2.0\ V$. This result demonstrates not only the possibility of SSDs to work as heterodyne detectors but also to generate higher harmonics [22].

In order to correctly perform the comparison with experimental measurements, we first calculate the matched MC power per diode, where the IF component is just extracted at $f = f_{\rm IF}$

$$P_{\rm MC}(f) = S_I(f) \times \Delta f \times {\rm Re}[Z(f)]. \quad (1)$$

Then, the IF power in dBm delivered to a 50 Ω load oscilloscope, $P(f_{\rm IF})$, is simply determined by taking into account the

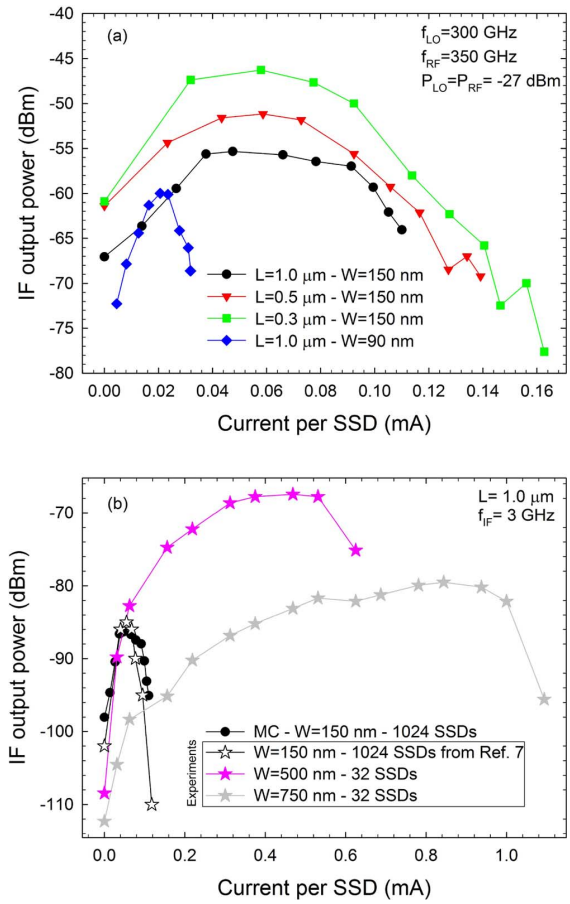

Fig. 6. (a) Matched IF output power obtained with Monte Carlo simulations using (1) at 50 GHz ($f_{\rm LO}$ = 300 GHz − $f_{\rm RF}$ = 350 GHz) versus the bias current for a single SSD with four geometries: $W = 150$ nm and three different lengths $L = 1.0, 0.5$ and 0.3 μm, and $L = 1.0$ μm − $W = 90$ nm. (b) Measured power of the IF signal versus bias current for arrays of SSDs with $L = 1.0$ μm and $W = 150, 500$ nm and 750 nm with $f_{\rm LO} = 300$ GHz and $f_{\rm RF} = 303$ GHz, so that IF is 3 GHz. The unmatched MC result, using (2), for an array of 1024 SSDs with $L = 1.0$ μm − $W = 150$ nm is also plotted in (b).

reflection coefficient, Γ (that depends on the number of SSDs), at the IF frequency

$$P(f_{\rm IF}) = 10 \times \log\left[\frac{P_{MC}(f_{\rm IF}) \times (1 - |\Gamma(f_{\rm IF})|^2)}{1\ \text{mW}}\right]. \quad (2)$$

Contrarily to direct detectors, which operate at equilibrium in order to reduce the excess noise (mainly $1/f$, appearing when $V \neq 0$), the efficiency of heterodyne detection (working around the IF, typically above the corner frequency of $1/f$ noise) can be improved by applying a DC bias to the devices. Fig. 6(a) shows the power at the IF obtained in the matched MC simulations using (1) for four devices: (A) $L = 1.0$ μm − $W = 150$ nm; (B) $L = 0.5$ μm − $W = 150$ nm; (C) $L = 0.3$ μm − $W = 150$ nm; and (D) $L = 1.0$ μm − $W = 90$ nm. To allow the comparison between different devices (for which simulations have been performed with the same AC excitation voltage, but providing different current), we have shifted the curves in order to compensate the different input power (and thus assuming LO and RF inputs of −27 dBm each). The simulations of SSDs with different geometries offer the following information: 1) shorter SSDs provide higher values of power at the IF and 2) the operation as heterodyne detectors is optimum when a DC bias corresponding to the knee of the *I–V* curve is applied. In contrast with the results of direct detection (Fig. 3), the reduction of the channel width does not enhance the output, even if the nonlinearity of the SSD is improved, since the current level is reduced. This happens because for heterodyne detection the output power is the magnitude of interest, instead of just the voltage, so that a significant current level is necessary. As such, the optimum value width must be chosen as a trade-off between a higher nonlinearity (obtained for narrow SSDs) and a large current level (obtained for large W).

Employing the THz set-up, see Fig. 1(b), two new geometries, $L = 1.0$ μm − $W = 500$ nm and $L = 1.0$ μm − $W = 750$ nm, have been tested and the experimental results are presented in Fig. 6(b), where an IF of 3 GHz has been chosen. Measurements were done using two sources of radiation: one was tuned from 0.22 to 0.32 THz and the second from 0.28 to 0.36 THz, thus providing an available zone for heterodyne detection from 280 to 320 GHz. The results for different W confirm the prediction of the simulations commented just before, showing that the performance of the SSD with $W = 500$ nm is much better than for $W = 150$ nm, even if the power matching is improved in the latter case by the use of an array of 16 bow-tie antennas with 64 SSDs on each (results extracted from [7]).

The amplitude of the LO and RF sources used in the MC simulations is $V_{\rm AC} = 0.25$ V. In order to perform the comparison between the experimental and simulated values for the array of 1024 SSDs of $L = 1.0$ μm and $W = 150$ nm we have taken into account that the simulated matched input power is about 2.5 dBm (corresponding to −27 dBm dissipated in each SSD) while the input power from the real sources is about −2 dBm, that is, 4.5 dB less. The good agreement between simulation and experiments shown in Fig. 6(b) has been obtained by including a value of 60 dB for the total losses in (2). They correspond partially to the electrical losses of the output connection that in [7] were estimated to be about 6 dB at the 3 GHz of the IF, the corrections related to a beam spot size much larger than the devices, the possible misalignment of the setup and the non-perfect coupling of the free space signal to the antenna connected to the SSDs. Therefore, we estimate these optical losses to be about 49.5 dB (= 60 − 6 − 4.5 dB), a very high value, which is yet consistent with the mentioned difficulties. Note that in this case $\mathrm{Re}[Z(f_{\rm IF})]$ and Γ in (1) is calculated using $16 \times 64 = 1024$ SSDs in parallel.

Note that some of the experimental results shown in this paper correspond to SSDs with wider channels than those reported in previous papers [6], [7], devoted to direct detection. The wider channel allows not only for an improved performance of SSDs as heterodyne detectors, but it also should allow for the onset of Gunn oscillations, thus opening the possibility to achieve emission [10] and detection with the same technology. Unfortunately, our prediction for THz generation has not yet been confirmed experimentally [23].

MC simulations allow to check the intrinsic limits of operation of our GaN-SSD as ultrahigh data-rate detectors. For that sake two types of MC simulations were performed using device A (Fig. 7): (i) keeping $f_{\rm LO}$ fixed to 250 GHz and sweeping $f_{\rm RF}$

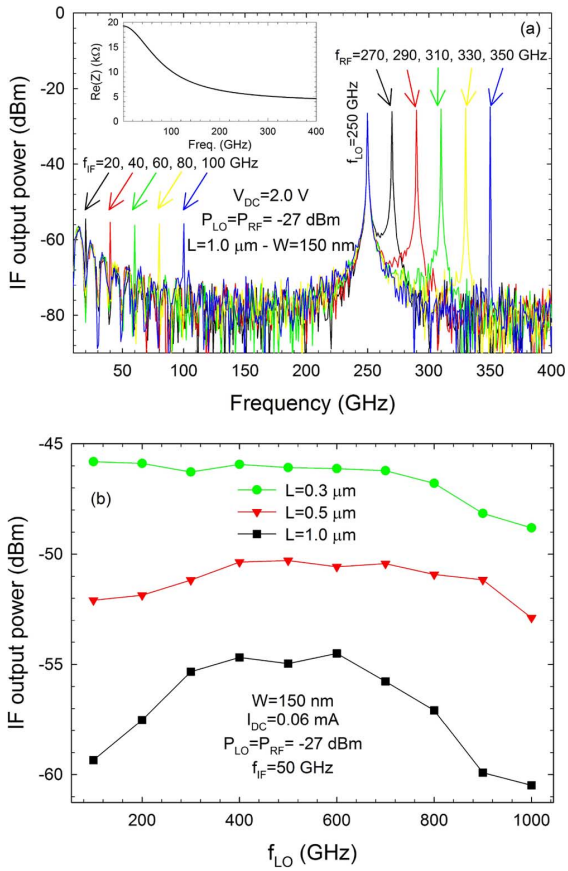

Fig. 7. Power spectra obtained using MC simulations and (1) (matched value) for different IF frequencies from 20 GHz up to 100 GHz for a single SSD with $L = 1.0\ \mu\text{m} - W = 150$ nm. Inset: $\text{Re}[Z(f)]$. (b) Matched IF power otput obtained using Monte Carlo simulation using (1) at 50 GHz versus the LO frequency from 0.1 to 1 THz for a single SSD with $W = 150$ nm and $L = 0.3, 0.5$ and $1.0\ \mu$m.

from 270 GHz up to 350 GHz in order to increase the IF from 20 to 100 GHz [Fig. 7(a)] and (ii) maintaining the same IF frequency of 50 GHz and increasing simultaneously the LO and RF frequencies, Fig. 7(b). In the first study, the simulations show that the amplitude of the IF signal is constant up to 100 GHz, with an intrinsic mixing conversion loss of about 30 dB, thus demonstrating no intrinsic frequency limitation. The second one shows that even if both frequencies approach the THz range (0.7–0.75 THz) the SSD with $L = 1.0\ \mu\text{m} - W = 150$ nm still operates correctly, showing only a slight intrinsic power roll-off. Moreover, such impressive intrinsic performances can be further improved by reducing the length of the SSDs. Fig. 7(b) shows a clear enhancement of the response at IF when the length of the SSDs is shortened down to 300 nm. Additionally, the roll-off observed at around 700 GHz for the LO in the SSD with $L = 1.0\ \mu$m is much improved for shorter L.

V. Conclusion

In summary, this paper demonstrates the functionalities of GaN SSDs as direct and heterodyne detectors and provides the guidelines for improving their performances at sub-THz frequencies. The experimental results of responsivity and output IF power are rather low, but they have been obtained on a setup which has not yet been optimized (optical and electrical losses are huge), so that a large room for improvement is expected. In fact, MC simulations foresee the possibility of increase of both the frequency of the carrier signals and the bandwidth of the heterodyne receiver. The different design rules to fabricate optimum devices for each application have been provided taking as a base the dependence of the responsivity and IF power on L and W obtained from MC simulations and confirmed by experimental measurements.

References

[1] O. Cojocari, B. Mottet, M. Rodriguez-Girones, S. Biber, L. Marchand, L.-P. Schmidt, and H. L. Hartnagel, "A new structural approach for uniform sub-micrometer anode metallization of planar THz Schottky components," *Semicond. Sci. Technol.*, vol. 19, pp. 537–542, 2004.

[2] R. Lai, X. B. Mei, W. R. Deal, W. Yoshida, Y. M. Kim, P. H. Liu, J. Lee, J. Uyeda, V. Radisic, M. Lange, T. Gaier, L. Samoska, and A. Fung, "Sub 50 nm InP HEMT Device with Fmax Greater than 1 THz," *IEDM Tech. Dig.*, p. 609, 2007.

[3] A. M. Song, M. Missous, P. Omling, A. R. Peaker, L. Samuelson, and W. Seifert, "Unidirectional electron flow in a nanometer-scale semiconductor channel: A self-switching device," *Appl. Phys. Lett.*, vol. 83, p. 1881, 2003.

[4] C. Balocco, S. R. Kasjoo, X. F. Lu, L. Q. Zhang, Y. Alimi, S. Winnerl, and A. M. Song, "Room-temperature operation of a unipolar nanodiode at terahertz frequencies," *Appl. Phys. Lett.*, vol. 98, p. 223501, 2011.

[5] C. Balocco, S. R. Kasjoo, L. Q. Zhang, Y. Alimi, and A. M. Song, "Low-frequency noise of unipolar nanorectifiers," *Appl. Phys. Lett.*, vol. 99, p. 113511, 2011.

[6] P. Sangaré, G. Ducournau, B. Grimbert, V. Brandli, M. Faucher, C. Gaquière, A. Íñiguez-de-la-Torre, I. Íñiguez-de-la-Torre, J. F. Millithaler, J. Mateos, and T. González, "Experimental demonstration of direct terahertz detection at room-temperature in AlGaN/GaN asymmetric nanochannels," *J. Appl. Phys.*, vol. 113, p. 034305, 2013.

[7] J. Torres, P. Nouvel, A. Penot, L. Varani, P. Sangar, B. Grimbert, M. Faucher, G. Ducournau, C. Gaquière, I. Íñiguez-de-la-Torre, J. Mateos, and T. González, "Non-linear nanochannels for room temperature terahertz heterodyne detection," *Semicond. Sci. Technol.*, vol. 28, p. 125024, 2013.

[8] A. Westlund, P. Sangaré, G. Ducournau, P.-A. Nilsson, G. Nilsson, C. Gaquière, L. Desplanque, X. Wallart, and J. Grahn, "Terahertz detection in zero-bias inas self-switching diodes at room temperature," *Appl. Phys. Lett.*, vol. 103, p. 133504, 2013.

[9] I. Íñiguez-de-la-Torre, H. Roddilla, J. Mateos, D. Pardo, A. M. Song, and T. González, "Terahertz tuneable detection in self-switching diodes based on high mobility semiconductors: InGaAs, InAs and InSb," in *J. Phys.: Conf. Series*, 2009, vol. 193, p. 012082.

[10] A. Íñiguez-de-la-Torre, I. Íñiguez-de-la-Torre, J. Mateos, T. González, P. Sangaré, M. Faucher, B. Grimbert, V. Brandli, G. Ducournau, and C. Gaquière, "Searching for THz Gunn oscillations in GaN planar nanodiodes," *J. Appl. Phys.*, vol. 111, p. 113705, 2012.

[11] H. Kazemil, G. Nagy, L. Tran, E. Grossman, E. R. Brown, A. C. Gossard, G. D. Boreman, B. Lail, A. C. Young, and J. D. Zimmerman, "Ultra sensitive ErAs/InAlGaAs direct detectors for millimeter wave and THz imaging applications," in *Int. Microw. Symp.*, 2007, pp. 1367–1370.

[12] E. R. Brown, A. C. Young, J. E. Bjarnason, H. Kazemi, J. Zimmerman, and A. C. Gossard, "Millimeter and sub-millimeter wave performance of an ErAs:InAlGaAs Schottky diode coupled to a single-turn square spiral," *Int. J. High Speed Electron. Syst.*, vol. 17, p. 383, 2007.

[13] S. Cherednichenko, A. Hammar, S. Bevilacqua, V. Drakinskiy, J. Stake, and A. Kalabukhov, "A room temperature bolometer for terahertz coherent and incoherent detection," *IEEE Trans. THz Sci. Technol.*, vol. 1, no. 2, p. 365, Nov. 2011.

[14] D. Glaab, S. Boppel, A. Lisauskas, U. Pfeiffer, E. Öjefors, and H. G. Roskos, "Terahertz heterodyne detection with silicon field-effect transistors," *Appl. Phys. Lett.*, vol. 96, p. 042106, 2010.

[15] G. C. Trichopoulos, L. Mosbacker, D. Burdette, and K. Sertel, "A broadband focal plane array camera for real-time THz imaging applications," *IEEE Trans. Antennas Propag.*, vol. 61, pp. 1733–1740, 2013.

[16] J. Mateos, B. G. Vasallo, D. Pardo, and T. González, "Operation and high-frequency performance of nanoscale unipolar rectifying diodes," *Appl. Phys. Lett.*, vol. 86, p. 212103, 2005.

[17] A. Íñiguez-de-la-Torre, I. Íñiguez-de-la-Torre, T. González, and J. Mateos, "Correlation between low frequency current-noise enhancement and high-frequency oscillations in gan-based planar nanodiodes: A Monte Carlo study," *Appl. Phys. Lett.*, vol. 99, p. 062109, 2011.
[18] A. Íñiguez-de-la-Torre, J. Mateos, D. Pardo, and T. González, "Monte Carlo analysis of noise spectra in self-switching nanodiodes," *J. Appl. Phys.*, vol. 103, p. 024502, 2008.
[19] J.-F. Millithaler, "Noise equivalent power in terahertz detectors based on semiconductor nanochannels," in *22 Int. Conf. on Noise and Fluctuations*, 2013, pp. 1–4.
[20] G. M. Dunn and M. J. Kearney, "A theoretical study of differing active region doping profiles for W-band (75–110 GHz) InP Gunn diodes," *Semicond. Sci. Technol.*, vol. 18, pp. 794–802, 2003.
[21] A. Cowley and H. Sorensen, "Quantitative comparison of solid-state microwave detectors," *IEEE Trans. Microw. Theory Techn.*, vol. MTT-14, no. 12, pp. 588–602, Dec. 1966.
[22] K. Y. Xu, X. F. Lu, A. M. Song, and G. Wang, "Terahertz harmonic generation using a planar nanoscale unipolar diode at zero bias," *Appl. Phys. Lett.*, vol. 92, p. 163503, 2008.
[23] J.-F. Millithaler, I. Íñiguez-de-la-Torre, A. Íñiguez-de-la-Torre, T. González, P. Sangaré, G. Ducournau, C. Gaquiére, and J. Mateos, "Optimized V-shape design of GaN nanodiodes for the generation of Gunn oscillations," *Appl. Phys. Lett.*, vol. 104, p. 073509, 2014.

Ignacio Íñiguez-de-la-Torre was born in Valladolid, Spain, in 1981. He received the B.S. and Ph.D. degrees in physics from the University of Salamanca, Salamanca, Spain, in 2004 and 2008, respectively.

He spent three months at the Institut d'Electronique, de Microèlectronique et de Nanotechnologies (IEMN), France in 2007, and another three months in the School of Electrical and Electronic Engineering in the University of Manchester, Manchester, U.K., in 2008. In 2009–2010, he was a Postdoctoral Research Fellow with the Department of Electrical and Computer Engineering at the University of Massachusetts in Lowell, MA, USA. He then joined the Electronics Group of the Department of Applied Physics at the University of Salamanca, Spain, first during 2010–2011, with a Postdoc contract in the EU project ROOTHz, and where he is currently a Lecturer. His main research interest is in the development of novel device concepts for terahertz (THz) data processing, detection and emission using both narrow and wide bandgap III–V semiconductors.

Carlos Daher was born in Thoum, Lebanon, in 1986. He received the B.S. degree and the M.S. degrees in physics and engineering from the University of Montpellier 2, France, in 2009 and 2012, respectively. In October 2012, he began working toward the Ph.D. degree for three years at the IES l'Institut d'Electronique laboratory at the University Montpellier 2, where he joined the terahertz team.

In March 2012, he was recruited for six months as an internship process engineer at the Commissariat of Atomic Energy CEA Grenoble, France, where he worked on the development of new chemical mechanical polishing process. He is currently working on the development of new detectors and emitters of THz radiations based on self-switching nanodevices. As part of his dissertation, he is a teacher with the faculty of science, the Department of Electronics, Electrical Engineering and Automation, University of Montpellier 2.

Jean-François Millithaler was born in Cherbourg, France, in 1979. He received the Ph.D. degree in electronics from the University of Montpellier 2, France, in 2006.

From 2007 to 2011, he worked as a research assistant in the Department of Engineering and Innovation of Salento University, in Italy. A part of his contract was related to the EU project BOND. In 2012, he worked on the EU project ROOTHz in the Electronic Group of the Department of Applied Physics at University of Salamanca, in Spain. In 2013, he obtained a research contract with the Labex Solstice at the University of Montpellier 2, France. His main research interest is dedicated to the study of electronic transport in III-V semiconductors for the development of novel device concepts for terahertz processing.

Jérémi Torres was born in Montpellier, France, in 1977. He received the Ph.D. degree in nanophotonics from the University of Montpellier, France, in 2004. From 2004 to 2005 he was postdoctoral fellow at the Laboratory for Photonics and Nanostructures, Marcoussis, France.

From 2005 to 2007 he was postdoctoral fellow then Assistant professor at the Institute of Electronics of the South. He is currently an Associate Professor of the Institute of Technology of Montpellier at the University of Montpellier, Montpellier, France. His research has been concerned with high-frequency electronics and transport in semiconductor materials and devices for generation, detection and applications of terahertz radiations. He is author and coauthor of about 100 scientific articles in refereed journals and conference proceedings.

Philippe Nouvel was born in Nimes, France, in 1975. He received the B.Sc. degree from the University of Montpellier II, Montpellier, France, in 2000, the M.Sc. degree in electronics, from the University of Montpellier in 2005, and is currently working toward the Ph.D. degree at the same university.

He joined the Institute de Radio Astronomie Millimetrique, Grenoble, France, in 2000, where he was with the Receiver Group on the millimeters systems. He is currently a Project Engineer with the Centre National de la Recherche Scientifique (CNRS), University of Lille 1, France. He is also currently with the Institute of Electronics of the South, University Montpellier II, Montpellier, France, where he is with the High-Frequency Investigation Group. His current research interests include detection and generation of terahertz radiations by optoelectronic systems.

Luca Varani was born in Carpi, Italy, in 1963. He received the Ph.D. degree in physics from the University of Modena, Italy, in 1993, and the Ph.D. degree in electronics from the University of Montpellier, France, in 1996 .

He is currently a Full Professor with the University of Montpellier and Head of the research group TeHO (TeraHertz, High-Frequency and Optics) of the Institute of Electronics and Systems (IES). His main research interest is in theoretical and experimental transport phenomena in semiconductor materials and devices with a special attention to the terahertz frequency range. He is author and coauthor of about 300 scientific articles in refereed journals and conference proceedings.

Paul Sangaré, photograph and biography not available at time of publication.

Guillaume Ducournau received the Diplome d'ingénieur from ESIGELEC, Rouen, France, in 2002, and the Ph.D. degree from the Université de Rouen in fiber optic communication systems using DPSK modulation schemes, in 2005.

In 2002, he worked in Canada on optical fiber Bragg gratings. Since 2007, he is an Assistant Professor at the IEMN/University of Lille 1 and Polytech'Lille Graduate School. He is involved mainly in the research of optoelectronic THz photomixers, for communication applications, THz instrumentation and imaging. He has 10 years of experience in the domain of

optical fibers technology and THz instrumentation. He is the coordinator of the French ANR project COM'TONIQ, dealing with quasi-optics THz links. He is author or co-author of more than 40 publications in peer-reviewed international journals or peer reviewed conferences proceedings. He has worked on several ANR and European projects (ITN "MITEPHO" and STREP "ROOTHz").

Christophe Gaquière received the Ph.D. degree in electronic from the University of Lille, France, in 1995.

He is currently Full Professor at the University of Lille (Polytech'Lille), and carries out his research activity at the Institut d'Electronique de Microélectronique et de Nanotechnology (IEMN). The topics concern design, fabrication, characterization and modeling of HEMT's and HBT devices. He works on GaAs, InP, metamorphic HEMT's and is currently involved in the GaN activities. His main activities are microwave characterizations (small and large signal between 1 and 500 GHz) in order to correlate the microwave performances with the technological and topology parameters. Today, his activities concern mainly the investigation of two-dimensional electronic plasmons and Gunn like effects for THz solid state GaN based detectors and emitters (HEMT and SSD), AlGaN/GaN nano-wires for microwave applications and MEMS activities based also on GaN. He was responsible for the microwave characterization part of the common laboratory between Thales TRT and IEMN focus on wide band gap semiconductor (GaN, SiC, and Diamond) from 2003 up to 2007. At the present time, he is in charge of the Silicon millimeter wave advanced technologies part of the common lab between ST microelectronics and IEMN. He is the author or co-author of more than 150 publications and 260 communications.

Tomás González (M'05–SM'07) was born in Salamanca, Spain, in 1967. He received the M.S. and Ph.D. degrees in physics from the University of Salamanca in 1990 and 1994, respectively.

Since 1991 he has been working in the Department of Applied Physics at the University of Salamanca, Spain, where he is currently Full Professor of Electronics. His main research activity is in the fields of high-frequency III–V transistors, microscopic modeling of electronic noise and development of novel THz device concepts based on ballistic transport. He is author or co-author of more than 125 refereed scientific journal papers and 170 conference presentations.

Dr. González serves on the Committees of several International Conferences (ICNF, EDISON).

Javier Mateos (M'09) was born in Salamanca, Spain, in 1970. He received the B.S. and Ph.D. degrees in physics from the University of Salamanca in 1993 and 1997, respectively.

Since 1993, he has been with the Department of Applied Physics of the University of Salamanca, becoming Associate Professor in 2000. He is presently coordinator of EU project ROOTHz aiming at fabricating THz emitters and detectors using semiconductor nanodevices. His present research interests also include the development of novel device concepts using ballistic transport and HEMTs based in both narrow and wide bandgap III–V semiconductors. He is author or co-author of more than 90 refereed scientific journal papers and 140 conference contributions.